Indian J. Phys. **75A** (5), 547-551 (2001)

IJP A
an international journal

Higher configurations-effects on the form factors in ^{9}Be and ^{19}F

R A Radhi
Department of Physics, College of Science, University of Baghdad, Baghdad, Iraq
E-mail : bagunv@uruklink.net

Received 26 February 2001, accepted 8 June 2001

Abstract : Core-polarization effect on electron scattering form factors are calculated for the low-lying levels of ^{9}Be (2.429 MeV, 5/2$^-$ and 6.76 MeV, 7/2$^-$) and for the ground state of ^{19}F. The calculation has been performed within the framework of microscopic theory that includes core-polarization effects. An over all agreement with the experimental data is obtained for the two low-lying levels in ^{9}Be considered in this work. Also the results agree very well with the intermediate maximum as well as the entire range of momentum transfer data for ^{19}F

Keywords : Low-lying levels of ^{9}Be, ^{19}F, core-polarization effects, electron scattering form factors

PACS Nos. : 25.30.-c, 21.60Cs, 27.20.+n

1. Introduction

Several types of theoretical calculations have been performed to describe the properties of *p*-shell and *sd*-shell nuclei. The multi-nucleon shell-model with mixed configurations is one of these theoretical models. According to this model, a closed core is assumed and the extra nucleons are distributed over a limited number of the higher orbits. This limited number of orbits form the model space. In spite of the success of the shell model on the static properties of nuclei in the region, it fails to describe electron scattering data at higher momentum transfer [1, 2]. The effect of higher configurations (configurations outside the model space) has to be considered to determine the success of shell model wave functions in describing electron scattering data. Such effects are usually called core-polarization effect [3]. The effect of core-polarization has been found to be essential in electron scattering on ^{12}C and ^{13}C[1]. Higher energy configurations have been studied for some 1*p*-shell nuclei, where the extended (0+2) $\hbar\omega$ model space was used [2,4,5]. These calculations did not include ^{9}Be. Extension of the model space to include the 2 $\hbar\omega$ configurations, improves the agreement with the transverse form factors in the beginning of the *p*-shell, but towards the end of the *p*-shell the situation deteriorates [2]. Cichocki *et al* [5] have found that only a 10% improvement was realized by extending the model space to include the 2 $\hbar\omega$ configurations in describing the form factors of ^{10}B. In the analysis of the longitudinal inelastic electron scattering form factors in ^{6,7}Li, Karataglidis and Brown [6] have used (0+2+4) $\hbar\omega$ wave functions and none of their results were able to reproduce the data at low momentum transfer, and the B(C2) value of each transition was underestimated by a factor of 2. The experimental data of the M1 elastic magnetic electron scattering on ^{19}F [7] display three maxima. The full *sd*-shell model calculation [8] were not able to reproduce the second maximum in the form factor. A large basis shell model calculations [7] using all orbits up to the $1f_{7/2}$ shell produced the second maximum, but no quantitative agreement were obtained. Core-polarization calculation [7] gave reasonable description of the data and showed that excitations from 1*s* to the 2*s* shell are mainly responsible for the appearance of the intermediate maximum. Their results showed that the high momentum transfer values enhanced with respect to the data. Bouten and Bouten [9] have used a projected Hatree-Fock function and reproduced the second maximum in the form factor, but the high *q*-data are underpredicted by a factor of two.

Cluster model calculations [10] reproduced the three maxima in the elastic magnetic form factor, but were unable to reproduce the form factors for the negative parity states.

The purpose of the present work is to use a microscopic theory, which connects the full model space wave functions with the particle-hole excitations from the core into the higher orbits. The modified surface delta interaction (MSDI) is used for the residual interaction. The two-body interaction of Cohen and Kurath [11] is used to generate the p-shell wave functions, while that of Wildenthal [12] is used to generate the sd-shell wave functions. The single-particle wave functions of the harmonic oscillator (HO) potential are used with size parameter b chosen so that the root mean square (rms) charge radius is reproduced. Free nucleon charges and current operators are used for all multipole components that contribute to the scattering.

The calculations include the $T = 1/2$ low-lying $J^\pi = 5/2^-$ (2.429 MeV) and $7/2^-$ (6.76 MeV) states in ^{9}Be, as well as the $1/2^+$ (0.0 MeV) state of ^{19}F.

2. Theory

The core-polarization effect on the form factors is based on a microscopic theory, which combines shell-model wave functions and configurations with higher energy as first order perturbations. The reduced matrix elements of the electron scattering operator T_Λ is expressed in terms of the residual interaction V_{res} as follows :

$$\langle \Gamma_f \| T_\Lambda \| \Gamma_i \rangle = \langle \Gamma_f \| T_\Lambda \| \Gamma_i \rangle_{MS} + \langle \Gamma_f \| \delta T_\Lambda \| \Gamma_i \rangle_{HC}, \quad (1)$$

where the states $|\Gamma_i\rangle$ and $|\Gamma_f\rangle$ are described by the model space wave functions. Greek symbols are used to denote quantum numbers in coordinate space and isospace, *i.e.* $\Gamma_i \equiv J_i T_i$, $\Gamma_f \equiv J_f T_f$ and $\Lambda \equiv J\,T$.

The model space (MS) matrix element is expressed as the sum of the product of the elements of the one body density matrix (OBDM) $\chi^{\Lambda}_{\Gamma_f \Gamma_i}(\alpha, \beta)$ times the single-particle matrix elements, and is given by [13]

$$\langle \Gamma_f \| T_\Lambda \| \Gamma_i \rangle_{MS} = \sum_{\alpha,\beta} \chi^{\Lambda}_{\Gamma_f \Gamma_i}(\alpha, \beta) \langle \alpha \| T_\Lambda \| \beta \rangle, \quad (2)$$

where α and β label are single-particle states (isospin is included) for the model space.

Similarly, higher energy configurations (HC) matrix element is written as

$$\langle \Gamma_f \| \delta T_\Lambda \| \Gamma_i \rangle_{HC} = \sum_{\alpha,\beta} \chi^{\Lambda}_{\Gamma_f \Gamma_i}(\alpha, \beta) \langle \alpha \| \delta T_\Lambda \| \beta \rangle. \quad (3)$$

According to the first-order perturbation theory, the higher-energy configuration single-particle matrix element is given by [14]

$$\langle \alpha \| \delta T_\Lambda \| \beta \rangle = \left\langle \alpha \| T_\Lambda \frac{Q}{E_i - H_0} V_{res} \| \beta \right\rangle + \left\langle \alpha \| V_{res} \frac{Q}{E_f - H_0} T_\Lambda \| \beta \right\rangle. \quad (4)$$

The operator Q is the projection operator onto the space outside the models pace. For the residual interaction V_{res}, we adopt the MSDI (14). E_i and E_f are the energies of the initial and final states, respectively. Eq. (4) is written as [14]

$$\langle \alpha \| \delta T_\Lambda \| \beta \rangle = \sum_{\alpha_1 \alpha_2 \Gamma} \frac{(-1)^{\beta+\alpha_2+\Gamma}}{e_\beta - e_\alpha - e_{\alpha_1} + e_{\alpha_2}} (2\Gamma+1) \begin{Bmatrix} \alpha & \beta \\ \alpha_2 & \alpha_1 \end{Bmatrix} \times \sqrt{(1+\delta_{\alpha_1 \alpha})(1+\delta_{\alpha_2 \beta})} \langle \alpha \alpha_1 | V_{res} | \beta \alpha_2 \rangle_\Gamma \langle \alpha_2 \| T_\Lambda \| \beta_1 \rangle + \text{Terms with } \alpha_1 \text{ and } \alpha_2 \text{ exchanged}, \quad (5)$$

where the index α_1 runs over particle states and α_2 over hole states and e is the single-particle energy. The core-polarization parts are calculated by keeping the intermediate states up to the $2p$-$1f$ shell. The hole states run over the $1s$ and $1p$ shells while the particle states run over the $2s$-$1d$ and $2p$-$1f$ shells.

3. Results and discussion

The 2.429 MeV (5/2) level in ^{9}Be :

Six multipole components contribute to the form factor : The M1, C2, E2, M3, C4 and E4 multipoles. Shell model calculations restricted to the $1p$-shell allow for a maximum multipolarity M3 in case of one-body operators. Due to the inclusion of the higher energy configurations, higher multipoles could show up. The total form factors are calculated for $\theta = 90^\circ$ and $\theta = 160^\circ$ and compared with the experimental data of Ref. [15]. In Figure 1, the model space ($1p$-shell orbits) calculation is shown as a dashed curve. In this model, only the model space wave functions are considered where five nucleons are distributed over the orbits $1p_{3/2}$ and $1p_{1/2}$. No contribution from the core or higher configurations is taken into account. The theoretical curve (dashed curve) underestimates the experimental data below $q = 2$ fm^{-1} in the $1p$-shell model space. The transition strength B(C2) is found to be equal to 9.46 e^{2}fm^4 in comparison with the experimental value of 45.7 ± 3.5 e^{2}fm^4 [16]. This discrepancy is greatly improved by introducing core-polarization by allowing particle-hole excitations from the $1s$ and $1p$ shells into the higher sd and $2p$-$1f$ shells. This model gives the value 41.1 e^{2}fm^4 for transition strength B(C2). This enhancement in the transition strength is reflected in the form factor as shown in Figure 1 (solid curve). The core polarization contribution is shown by

the dotted curve. The experimental data are very well explained throughout the entire momentum transfer region studied here.

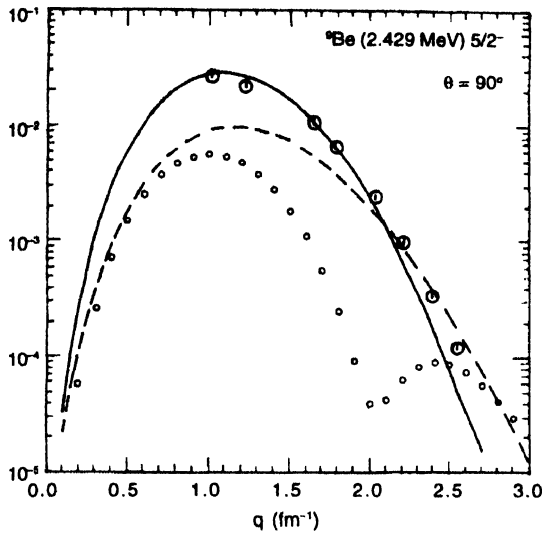

Figure 1. Total form factor for the electroexcitation of the $J^\pi = 5/2^-$, $T = 1/2$ level in ^{9}Be at 2.429 MeV. The calculation in the 1p-shell model space is indicated by the dashed curve and the core-polarization effect (higher energy configurations) is indicated by the dotted curve. The total form factor including core polarization effect is shown by the solid curve. The data are taken from Ref. [15].

In Figure 2, the transverse (M1 + E2 + E4) and longitudinal (C2 + C4) multipole contributions are shown where the Coulomb form factor dominates the scattering. The total form factors are compared with the experimental data for $\theta = 90°$ and for $\theta = 160°$ (Solid and dashed curves, respectively). The E4 contribution turned out to be less than 10^{-6} while the C4 contribution is less than 10^{-4} over the entire momentum transfer region studied here.

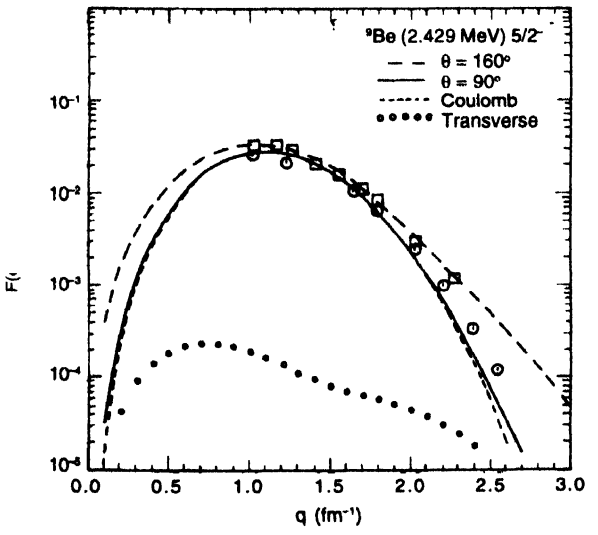

Figure 2. Total form factor including core polarization effect for the electroexcitation of the $J^\pi = 5/2^-$, $T = 1/2$ level in ^{9}Be at 2.429 MeV. The solid curve is the calculation for $\theta = 90°$ in comparison with the experimental data (Circles) of Ref. [15]. The dashed curve is the calculation for $\theta = 160°$ in comparison with the experimental data (squares) of Ref. [15]. The Transverse and Coulomb multipole components are also shown as indicated.

The 6.76 MeV (7/2$^-$) level in ^{9}Be :

The total form factors are calculated for $\theta = 160°$ for which the data are available. Figure (3) shows the total form factors calculated with the 1p-shell model space (dashed curve) and with the core-polarization effects (solid curve). The core-polarization contribution is shown by the dotted curve. The data are reasonably explained with the core-polarization calculation which enhances the form factor. In Figure 4, the transverse (E2+E4+M5) and longitudinal (C2+C4) multipole

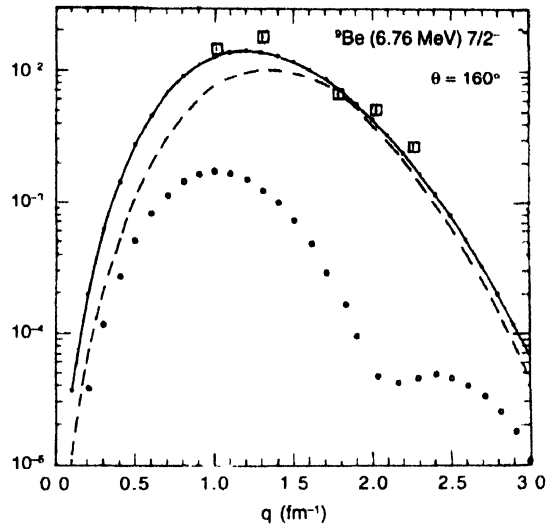

Figure 3. Total form factor for the electroexcitation of the $J^\pi = 7/2^-$, $T = 1/2$ level in ^{9}Be at 6.76 MeV. The same labeling as in Figure 1 is used. The data are taken from Ref. [15].

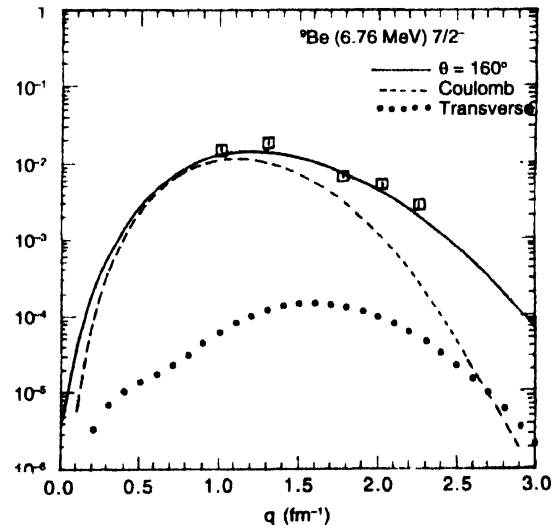

Figure 4. Total form factor including core-polarization effect for the electroexcitation of the $J^\pi = 7/2^-$, $T = 1/2$ level in ^{9}Be at 6.67 MeV. The solid curve is the calculation for $\theta = 160°$ in comparison with the experimental data (squares) of Ref. [15]. The transverse and Coulomb multipole components are also shown as indicated.

contributions are shown where the Coulomb form factor dominates the scattering. The E4 and M5 contributions turned out to be less than 10^{-6} while the C4 contribution is less than 10^{-4} over the entire momentum transfer region studied here. The single-particle wave functions of HO potential are used with size parameter 1.62 fm.

The $1/2^+$ ground state of ^{19}F :

The calculated M1 form factor for the ground $1/2^+$ state of ^{19}F failed to account for the second maximum, when the shell-model calculations in the full $2s$ $1d$-configuration space were employed [7]. M1 form factor is shown in Figure 5 (solid curve) using the full *sd* configuration space with Wildenthal interaction for the two particle matrix elements in comparison with the experimental data [7]. One feature of the data quoted is that they exhibit large error bars in the intermediate region. The calculated form factor shows a good agreement with the experimental data in the regions of $q < 1$ fm^{-1} and slightly overestimates the data for $q >$ 1.5 fm^{-1}. The form factor fails to describe the data in the region $1 < q < 1.5$ fm^{-1}, where the experimental data exhibit a second maximum. Core-polarization effects are calculated by perturbation theory by allowing particle-hole excitations from the $1s$ and $1p$ shells that form the closed ^{16}O core into the higher $2s$-$1d$ shell. These calculations are based on the shell model in the full *sd*-shell space, with the same OBDM elements used for the model space calculations. This correction is shown in Figure 5 as a dotted curve. The M1 form factor including the core-polarization correction is shown in Figure 6 (solid curve) in comparison with the model space result (dashed curve). The form factor is slightly reduced around its third maximum and becomes closer to the experimental data in this region. The second maximum is quite well reproduced by this correction. Although all possible particle-hole excitations are considered, it is found that the main contribution to the core-polarization correction comes from the $1s$ to $2s$ excitation. Use of effective operators to reproduce the measured static properties (at the photon $q = 0$ point), can not be considered as a core-polarization correction, since the q-dependent form factor deviates from experiment at non-zero q. The single-particle wave functions of the HO potential are used with size parameter $b = 1.833$ fm, so that the rms charge radius of ^{19}F is reproduced [17].

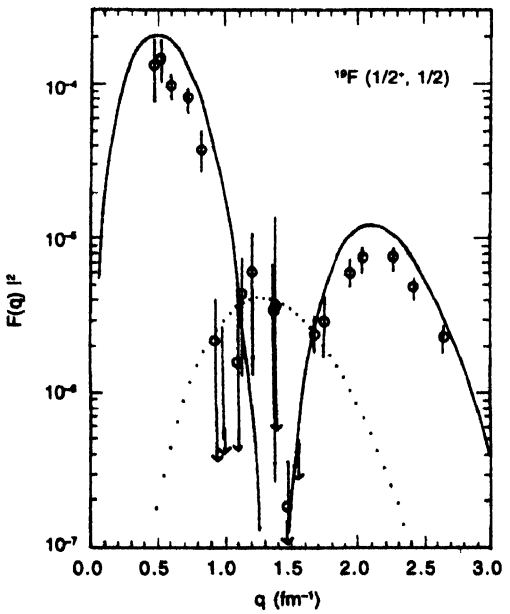

Figure 5. Magnetic M1 form factor for the ground $1/2^+$ state of ^{19}F. The solid curve represents the calculation with the full *sd*-shell model wave functions. The dotted curve represents the core-polarization correction. The data are taken from Ref. [7].

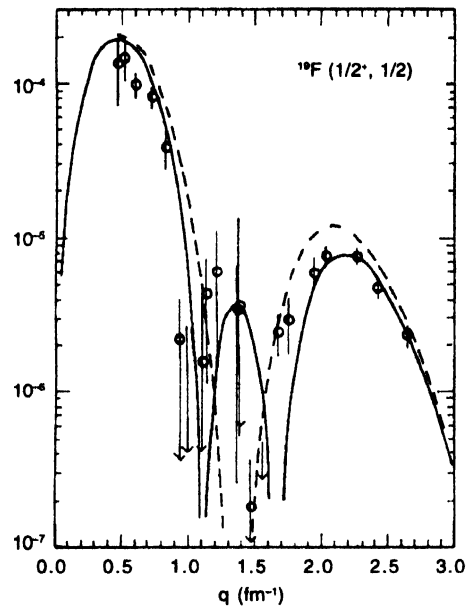

Figure 6. magnetic M1 form factor for the ground $1/2^+$ state of ^{19}F calculated with full *sd*-shell model wave functions (dashed curve) and with full *sd*-shell wave functions + core polarization (solid curve). The data are taken from Ref. [7].

Core-polarization is essential to electromagnetic transition strength and form factors in *p*-shell region and *sd*-shell region when combined with full *p*-shell and *sd*-shell configurations, respectively.

References

[1] T Sato, K Koshigiri and H Ohtsubo *Z. Phys. A- Atoms and Nuclei* **320** 507 (1985)

[2] J G L Booten and A G M van Hees *Nucl. Phys.* **A 569** 510 (1994)

[3] A Bohr and B Mottelson *Nuclear Structure* **Vol 2** (New York W A. Benjamin) (1975)

[4] T Sato, N Odagawa, H Ohtsubo and T S H Lee *Phys. Rev.* C 49 776 (1994)

[5] A Cichocki, J Dubach, R S Hicks, G A Peterson, C W de Jager, H de Vries, N Kalantar-Nayestanaki and T Sato *Phys. Rev.* C 51 2406 (1995)

[6] S Karataglidis and B A Brown *Phys. Rev.* **C55** 2826 (1997)

[7] A J H Donne, G Van Middelkoop, L Lapikas, T Suzuki, P W M Glaudemans and D Zwartz *Nucl. Phys.* **A455** 453 (1986)

[8] B A Brown, B H Wildenthal, C F Williamson, F N Rad, S Kowalski, H Cronnel and J T O Brien *Phys. Rev.* **C32** 1127 (1985)

[9] M Bouten and M C Bouten *Nucl. Phys.* **A459** 253 (1986)

[10] T Sakuda *Prog. Theo. Phys.* **87** 1159 (1992)

[11] S Cohen and D Kurath *Nucl. Phys.* **73** 1 (1965)

[12] B H Wildenthal *Progress in Particle and Nuclear Physics*, (ed) D H Wilkinson (London : Pergamon) **11** p 5 (1984)

[13] T W Donnelly and I Sick *Rev. Mod. Phys.* **56** 461 (1984)

[14] P J Brussaard and P W M Glaudemans *Shell Model Applications in Nuclear Spectroscopy* (Amsterdam North Holland) p351 (1977)

[15] R W Lourie (Private communication)

[16] N Ensslin, W Bertozzi, S Kowalski, C P Sargent, W Turchinetz, C F Williamson, S P Fivozinsky, J W Lightbody, Jr and S Penner *Phys. Rev.* **C 9** 1705 (1974)

[17] L A Schaller, T Dubler, K Kaesser, G A Rinker, B Robert-Tissot, L Schellengberg and H Scheneuwly *Nucl Phys* **A300** 225 (1978)